Z. Kristallogr. Suppl. **26** (2007) 489-494

Defect structure examination of Sn-doped indium oxide (ITO)

J. Popović[1], E. Tkalčec[2,*], B. Gržeta[1], C. Goebbert[3], V. Ksenofontov[4] and M. Takeda[5]

[1] Ruđer Bošković Institute, P.O. Box 180, HR-10002 Zagreb, Croatia
[2] Faculty of Chemical Engineering and Technology, University of Zagreb, Marulićev trg 20, HR-10000 Zagreb, Croatia,
[3] ItN Nanovation, D-38820 Halberstadt, Germany
[4] Johannes Gutenberg-Universität, Staudinger Weg 9, D-55099 Mainz, Germany
[5] Faculty of Science, Toho University, Funabashi, Chiba 274-8510, Japan

[*] Contact author: E. Tkalčec; e-mail: etkalcec@fkit.hr

Keywords: Indium tin oxide (ITO), X-Ray powder diffraction, Mössbauer spectroscopy, Rietveld method, Fitting methods

Abstract. Tin-doped indium oxide (ITO) samples with doping level up to 12.3 at% Sn were prepared by a sol-gel technique and characterised by X-ray powder diffraction as well with ^{119}Sn-Mössbauer spectroscopy. Diffraction patterns indicated that all samples were cubic, space group $Ia\bar{3}$, and isostructural with In_2O_3. Diffraction lines were broadened, the line broadening increased with tin content. The unit-cell parameter increased with tin doping level up to 7.8 at% Sn and decreased at higher levels. This behaviour of the unit-cell parameter indicated that the tin substitution for indium on B and D sites of the original In_2O_3 structure is non-uniform and depends on tin content. Rietveld structure refinement showed the presence of interstitial oxygen in the Sn-doped samples. The position of interstitial oxygen indicated the D site preference for tin at low tin doping level, and subsequent increase in the B site occupancy with the increase in tin content. ^{119}Sn-Mössbauer spectroscopy revealed that incorporated tin resided equally sites B and D for 7.8 at% Sn. Below that doping level the preference for tin to occupy D site was noticed, while for doping level higher than 7.8 at% Sn the B site was preferred.

Introduction

Tin doped In_2O_3 (ITO) is one of the most commonly used transparent conducting oxides. It is used in various commercial applications: transparent electrodes in solar collectors and solar cells, transparent heating elements for aircraft windows, for antistatic coating on instrument windows and in production of flat-panel displays (LCD and touch-screen) [1]. It is not surprising that ITO found application in wide range of technologies, since it offers the best

available performance in terms of transmissivity and conductivity, combined with excellent environmental stability, reproducibility and good surface morphology [2]. Indium oxide crystallizes in a cubic bixbyite–type structure in space group $Ia\bar{3}$ [3]. It has 80 atoms in its unit cell, where 32 sites are occupied by cations in two non-equivalent six-fold coordinated sites. One fourth of cations is located on trigonally compressed octahedral sites referred to as B sites, while the remaining three fourths of cations are located on highly distorted octahedral D sites. Indium atoms, on both B and D sites, reside at the centre of a distorted cube with six corners occupied by oxygen atoms, while the remaining two corners are empty. In the case of the B site, oxygen vacancies are located along body diagonal, while in the case of the D site they are located along a face diagonal. With tin doping a charge imbalance is created due to a different valence of indium and tin ions. The charge imbalance can be compensated by incorporation of interstitial oxygen atoms, O_i. Both tin cations and interstitial oxygen anions are considered as defects in indium oxide structure. Franck and Köstlin proposed the existence of clustered defects rather than isolated point defects in order to explain the conductivity of ITO [4]. These clusters of defects can be positive, negative or neutral, where overall charge depends on the stoichiometry of the cluster. Despite of the widespread use of ITO, its structure is still not completely understood, nor the correlation between the structure and its physical properties. Recently, several structural studies on ITO have been reported by Nadaud et al. [5], Binczycka et al. [6] and Gonzales et al. [7,8]. Results based on TOF neutron diffraction, EXAFS and Mössbauer spectroscopy indicate that tin prefers to occupy B sites in the structure of In_2O_3, rather than D site. However, first principle density functional theory calculations performed by Warschkow et al. [9-11] suggested that preferred substitution of Sn^{4+} for In^{3+} should be expected on D sites. The present work reports the structural characterisation of nanocrystalline ITO samples by means of X-ray powder diffraction (XRD) and ^{119}Sn Mössbauer spectroscopy.

Experimental

The powder samples of pure In_2O_3 and ones doped with tin in the amounts of 2.1, 4.0, 6.0, 7.8, 9.7, 11.1 and 12.3 at% (the samples S0-S7) were prepared by a sol-gel technique from $InCl_3$ and $SnCl_4$ reagent grade chemicals, followed by thermal treatment at 300 °C for 2 h. The tin content in the samples were determined by means of PIXE (Particle Induced X-ray Emission) spectroscopy, using a nuclear microprobe facility with 3MeV proton beam and semiconductor Si(Li) X-ray detector [12]. The *K*-series of emitted X-ray radiation from thin powder samples was used for the analysis.

Structural changes due to tin incorporation in indium oxide lattice were studied by X-ray diffraction (XRD) at room temperature using a Philips MPD 1880 counter diffractometer with Cu $K\alpha$ radiation. UNITCELL program [13] and WPPF program [14] were used for precise determination of the unit-cell parameter, using silicon as an internal standard. Rietveld structure refinement [15] was performed for all samples using the program X′pert HighScore Plus [16]. In the case of ITO samples, the difference between X-ray scattering factors for In^{3+} and Sn^{4+} is too small to distinguish between tin and indium cations. Nevertheless, the Rietveld refinement was useful for the determination of the content and position of the interstitial oxygen atoms, which could indicate the mode of tin incorporation in the original In_2O_3 structure. The local environment of tin in ITO samples was investigated by ^{119}Sn

Mössbauer spectroscopy**.** Spectra were recorded at room temperature for samples S2, S3, S4 and S7 by conventional transmission Mössbauer spectrometer, using the $Ca^{119m}SnO_3$ source. They were analyzed using a transmission integral method [17].

Results and discussion

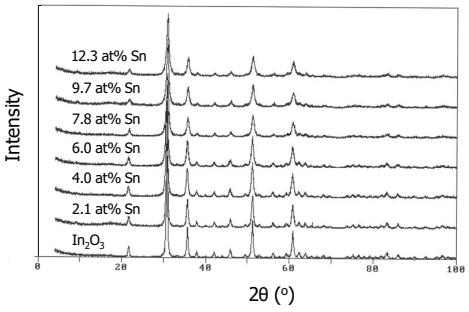

Figure 1. XRD patterns Sn-doped In_2O_3 samples.

Characteristic parts of XRD patterns of the as-prepared samples are presented in figure 1. XRD patterns revealed that all prepared samples have In_2O_3 type structure [3]. No impurities were detected in the samples. Diffraction lines were broadened indicating the nanosized crystallites. The line broadening increased with tin content. Line broadening analysis showed that crystallites in the samples decreased from 25 (for S0) to 17 nm (for S7).

Unit-cell parameter increased with tin doping level up to 7.8 at% and decreased at higher levels, as seen in figure 2. Such behaviour of the unit-cell parameter indicated that Sn substitution for In on B and D sites of the structure is non-uniform and depends on Sn content.

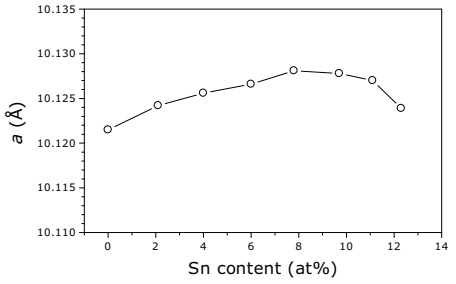

Figure 2. Lattice parameter of Sn-doped In_2O_3 samples.

The structure reported by Marezio [3] for pure In_2O_3 was used as a starting model for Rietveld structure refinement. In the case of Sn-doped In_2O_3, vacant anion sites in the In_2O_3 structure provide a space to accommodate excess oxygen, which compensate the charge imbalance. These sites are denoted as interstitial oxygen sites [5]. The positions of interstitial oxygen sites are well described by Warschkow et al. [11] as follows. Oxygen vacancies in In_2O_3 structure are located on "16*c* axis", (axis parallel to [111]) and are tetrahedrally coordinated by four cations. One B cation is located on 16*c* axis at $x=y=z=0.250$ (all positions given in lattice units), and three D cations are located in the plane which intersects 16*c* axis at the position 0.072. Given this geometry, the position of interstitial oxygen can be estimated by choosing a point on 16c axis which is equally distant to all four cations. That point is at $x=y=z=0.116$, and it is referred as an "ideal" position. So, the structural model for refinement of ITO structure was that of undoped In_2O_3 with addition of the "ideal" interstitial oxygen position at 16*c* (0.116, 0.116, 0.116) [11]. During the Rietveld refinement, the ther-

mal parameter of the interstitial oxygen ions O_i was constrained to be the same as that of the lattice oxygen because it is not possible to refine temperature factors for sites whose occupancy is small [7]. The results of Rietveld refinement for undoped In_2O_3 and samples S1-S7 are given in table 1.

Table 1. The results of Rietveld structure refinement for the samples S0-S7. R_p and R_{wp} are the discrepancy factors which characterize a quality of fitting result [18].

S	R_p	R_{wp}	Atom	Wyc	Occ.	x	y	z	B_{iso}(Å^2)
S0	0.0496	0.0723	In1	8b	1	0.250000	0.250000	0.250000	0.29(3)
			In2	24d	1	0.46671(5)	0.000000	0.250000	0.46(2)
			O1	48e	1	0.3915(4)	0.1557(4)	0.3816(4)	0.36(9)
S1	0.0547	0.0783	In1	8b	1	0.250000	0.250000	0.250000	0.24(3)
			In2	24d	1	0.46687(5)	0.000000	0.250000	0.36(2)
			O1	48e	1	0.3910(5)	0.1554(4)	0.3812(5)	0.27(9)
			O_i	16c	0.02(1)	0.08(1)	0.08(1)	0.08(1)	0.27(9)
S2	0.0517	0.0727	In1	8b	1	0.250000	0.250000	0.250000	0.24(3)
			In2	24d	1	0.466824)	0.000000	0.250000	0.38(2)
			O1	48e	1	0.3898(5)	0.1557(3)	0.3800(4)	0.51(1)
			O_i	16c	0.038(2)	0.08(2)	0.08(2)	0.08(2)	0.51(1)
S3	0.0557	0.0777	In1	8b	1	0.250000	0.250000	0.250000	0.24(3)
			In2	24d	1	0.46705(5)	0.000000	0.250000	0.50(2)
			O1	48e	1	0.3898(5)	0.1563(4)	0.3813(5)	0.54(7)
			O_i	16c	0.056(4)	0.083(7)	0.083(7)	0.083(7)	0.54(7)
S4	0.0567	0.0793	In1	8b	1	0.250000	0.250000	0.250000	0.37(3)
			In2	24d	1	0.46753(6)	0.000000	0.250000	0.43(2)
			O1	48e	1	0.3896(6)	0.1559(4)	0.3812(6)	0.67(8)
			O_i	16c	0.073(6)	0.087(3)	0.087(3)	0.087(3)	0.67(8)
S5	0.0568	0.0772	In1	8b	1	0.250000	0.250000	0.250000	0.34(4)
			In2	24d	1	0.46761(6)	0.000000	0.250000	0.46(3)
			O1	48e	1	0.3888(5)	0.1557(4)	0.3811(5)	0.66(6)
			O_i	16c	0.105(3)	0.089(4)	0.088(4)	0.088(4)	0.66(6)
S6	0.0587	0.0798	In1	8b	1	0.250000	0.250000	0.250000	0.31(4)
			In2	24d	1	0.46782(7)	0.000000	0.250000	0.43(3)
			O1	48e	1	0.3892(6)	0.1556(5)	0.3833(7)	0.59(8)
			O_i	16c	0.111(4)	0.091(5)	0.091(5)	0.091(5)	0.59(8)
S7	0.0548	0.0756	In1	8b	1	0.250000	0.250000	0.250000	0.34(5)
			In2	24d	1	0.46841(7)	0.000000	0.250000	0.49(3)
			O1	48e	1	0.3884(6)	0.1554(5)	0.3817(7)	0.61(7)
			O_i	16c	0.130(6)	0.093(4)	0.093(4)	0.093(4)	0.61(7)

It was noticed that atomic coordinates for interstitial oxygen atom were shifted from the "ideal" towards much smaller *x,y,z* values with decreasing dopant content, which according to [11] indicates a preference of Sn for the D site. However, it was found that *x,y,z* values for O_i increased with the increase in Sn content but still remained below $x=y=z=0.116$, implicating the change in D/B occupancy ratio in favour to B site. From Rietveld refinement the chemical formulas for ITO samples were obtained, and the general formula for our ITO samples follows: $(In_{1-x}Sn_x)_2O_3(O_i)_x$, where x is the occupancy of the interstitial oxygen site. According to that formula and found content of interstitial oxygen, the Sn content in ITO samples was determined. The results of Sn content in ITO samples obtained by Rietveld refinement and by PIXE analysis were equal within the standard deviation.

The ^{119}Sn-Mössbauer spectroscopy results for selected ITO samples is shown in figure 3. The Mössbauer spectra were resolved as two doublets, due to the presence of two non-equivalent crystallographic cation sites in the In_20_3 structure.

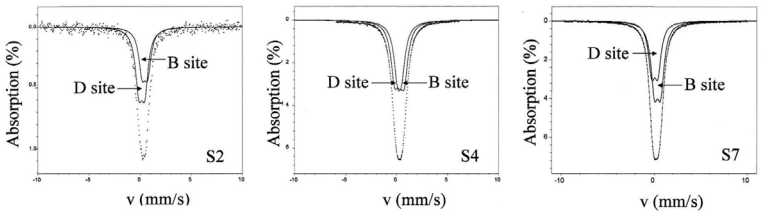

Figure 3. ^{119}Sn-Mössbauer spectra of the samples S2, S4 and S7.

The interpretation of the spectra as two doublets was suggested by Binczycka [6]. The ^{119}Sn Mössbauer parameters for samples S2, S3, S4 and S7 are listed in table 2. Isomer shift values (δ) in all ITO samples indicated that tin is present only in the Sn(IV) oxidation state.

Table 2. ^{119}Sn-Mössbauer parameters for selected ITO samples.

Sample	D site			B site		
	δ (mm s^{-1})	e^{2}qQ (mm s^{-1})	A_D (%)	δ (mm s^{-1})	e^{2}qQ (mm s^{-1})	A_B (%)
S2	0.16(6)	0.58(4)	64(4)	0.47(6)	0.55(5)	36(4)
S3	0.17(6)	0.59(1)	61(2)	0.46(6)	0.60(1)	39(2)
S4	0.12(2)	0.63(5)	50(2)	0.43(2)	0.61(5)	50(2)
S7	0.06(2)	0.65(4)	42(3)	0.36(2)	0.66(4)	58(3)

The values of quadrupole splitting (e^2qQ) for both doublets increased with tin content, suggesting major changes in tin environment as tin content increases. The main difference in Mössbauer spectra was observed in relative area ratio of two doublets. For samples up to 7.8 at% Sn the relative area (A_D) of D doublet was larger than relative area (A_B) of B doublet ($A_D+A_B=100\%$), indicating preferred substitution of Sn on D sites. For the sample with 7.8 at% the relative area for D and B doublets were equal, while for samples above 7.8 at% Sn an opposite tendency was observed, indicating B site as the preferred Sn-doping site.

Our results, based on both Rietveld refinement and Mössbauer spectroscopy, agree very well with first-principles density functional theory calculations performed by Warschkow et al. [9-11]. They found that calculated cluster forming energy was minimal (-1.91 eV) for cluster which consists of interstitial oxygen and two tin cations on D site, which suggested the D site as preferred doping site for lightly-doped samples. Based on results of that study, the explanation for change of unit cell parameter as a function of tin doping level can be proposed. The lattice parameter is influenced by three effects:

(*i*) increase of repulsive force between cations arising from effective charge of tin,

(*ii*) introduction of interstitial oxygen in the structure,

(*iii*) formation of neutral clusters that partially shield the neighboring charge.

For lower doping levels (up to 7.8 at% Sn) the effects (*i*) and (*ii*) are dominant, while at Sn doping levels above 7.8 at% Sn the (*iii*) effect dominates.

Concluding remarks

Tin substitution for indium on B and D sites of In_2O_3 structure is non-uniform and depends on tin content in ITO.

The interstitial oxygen sites in Sn-doped In_2O_3 structure are significantly displaced from the "ideal" four-fold position. The shift of the interstitial oxygen position caused by tin incorporation indicates the preference of tin to occupy D sites for low doping levels, and subsequent change in the D/B occupancy ratio in favour of the B site with the increase in tin doping level. Mössbauer spectroscopy confirmed that.

References

1. Chopra, K.L., Major, S., Pandya, D.K., 1983, *Thin Solid Films,* **102**, 334.
2. Lewis, B.G., Paine, D.C., 2000, *MRS Bull.*, **25**, 22.
3. Marezio, M., 1966, *Acta Cryst*., **20**, 723.
4. Franck, G., Köstlin, H., 1982, *Appl. Phys. A.,* **27**, 197.
5. Nadaud, N., Lequeux, N., Nanot, M., Jove, J., Roisnel, T., 1998, *J. Sol. St. Chem*., **135**, 140.
6. Binczycka, H., Uhrmacher, M., Ellidrisi-Moubtassim, M.L., Jumas, J.C., Schaaf, P., 2005, *Phys. Stat. Sol.,* **242**, 1100.
7. Gonzales, G.B., Cohen, J.B., Hwang, J.H., Mason, T.O., Hodges, J.P., Jorgensen, J.D., 2001, *J. Appl. Phys.,* **89**, 2550.
8. Gonzales, G.B., Mason, T.O., Quintana, J. P., Warschkow, O., Ellis, D. E., Hwang, J.H., Hodges, J.P., Jorgensen, J.D., 2004, *J. Appl. Phys.,* **96**, 3912.
9. Warschkow, O., Ellis, D.E., Gonzales, G.B., Mason, T.O., 2003, *J. Am. Ceram. Soc,* **86**, 1707.
10. Warschkow, O., Ellis, D.E., Gonzales, G.B., Mason, T.O., 2003, *J. Am. Ceram. Soc,* **86**, 1700.
11. Warschkow, O., Miljacic, Lj., Ellis, D.E, Gonzales, G.B., Mason, T.O., 2006, *J. Am. Ceram.Soc,* **89**, 616.
12. Jakšić, M., Bogadanović, I., Dujmić, D., Fazinić, S., Tadić, T., 1996, *Strojarstvo,* **38**, 279.
13. Toraya, H., 1993, *J. Appl. Cryst*., **26**, 583.
14. Toraya, H., 1986, *J. Appl. Cryst.,* **19**, 440.
15. Rietveld, M., 1996, *J. Appl. Cryst.,* **2,** 65.
16. X'Pert HighScore Plus Program, version 2.1. PANalytical, 2004, Almelo, The Netherlands.
17. Shenoy, G.K., Friedt, J.M., Maletta, H., Ruby, S.L., in *Mössbauer Effect Methodology*, 1974, Vol. 9, edited by I.J. Gruverman, C.W. Seidel, D.K. Dieterly, New York: Plenum Press, p. 277.
18. Young, R.A., Prince, E., Sparks, R.A., 1982, *J. Appl. Cryst*., **5**, 357.